J. Fluid Mech. (2017), *vol.* 821, *pp.* 582–594.
doi:10.1017/jfm.2017.213

Scaling of small vortices in stably stratified shear flows

Kengo Deguchi†

School of Mathematical Sciences, Monash University, VIC 3800, Australia

(Received 13 December 2016; revised 2 April 2017; accepted 2 April 2017;
first published online 25 May 2017)

The present paper treats the large Reynolds number scaling of coherent structures in stably stratified flows sheared between two horizontally placed walls. Three-dimensional steady solutions are used to confirm the theoretical scaling. For small values of the Richardson number, the previously known scaling based on the vortex–wave interaction/self-sustaining process is found to give excellent predictions of the numerical results. When the Richardson number is increased, the maximum size of the vortices is limited by the Ozmidov scale. The largest possible Richardson number to sustain the vortices is predicted to be of order unity when the typical length scale of the vortices reaches the Kolmogorov scale. The minimum-scale vortices are governed by unit Reynolds number Navier–Stokes equations.

Key words: high-speed flow, nonlinear instability, stratified flows

1. Introduction

Stably stratified parallel shear flows have been much studied owing to their deep relation to geophysics. A number of authors have studied the evolution of the velocity and density fields for various model background flows. One of the typical models concerned is the free-shear layer, where Kelvin–Helmholtz or Holmboe instabilities develop to enhance mixing and heat transfer; see the review paper by Peltier & Caulfield (2003). On the other hand, for a homogeneous shear layer, less theoretical progress has been made, since there is no available linear instability mechanism. The stability problem of linearly stable flows must be tackled by a three-dimensional nonlinear framework, and thus massive numerical simulations have been performed; see Portwood *et al.* (2016) and references therein. The computational results have repeatedly shown that the stratification drastically affects the flow regime: with increasing Richardson number, typically large-scale structures such as streaks break down into small-scale vortex patches.

In order to further the theoretical understanding of the sheared convection flows between two walls, Busse and his colleagues have employed bifurcation theory, solving for equilibrium solutions of the governing equations by Newton's method. Of particular relevance to the present work is that by Clever & Busse (1992), where plane Couette flow heated above or below is treated. They showed that nonlinear three-dimensional steady solutions exist over a wide range of stable and unstable density distributions, across the isothermal case. Their isothermal solution coincides

† Email address for correspondence: kengo.deguchi@monash.edu

with the nonlinear plane Couette flow solution found by Nagata (1990). The discovery of nonlinear equilibrium solutions in linearly stable flows is a cornerstone of nonlinear theory in transitional and fully developed turbulence; see Kawahara, Uhlmann, & Van Veen (2012).

Here we are concerned with the Reynolds number scaling of vortex structures in stably stratified flows, and its validation using the nonlinear equilibrium solutions. Recently Hall & Sherwin (2010) showed for isothermal plane Couette flow that the large Reynolds number asymptotic theory developed by Hall & Smith (1991), called vortex–wave interaction (VWI), gives excellent predictions of the Navier–Stokes computation of nonlinear solutions. Subsequently Eaves & Caulfield (2015) investigated the transition to turbulence in stably stratified plane Couette flow by the direct adjoint looping (DAL) method. This method can identify the input that maximises the relative kinetic perturbation energy at a certain target time. When the Richardson number is small, it was found that the computed trajectory remains in a quasi-steady state reminiscent of the VWI state. For larger Richardson numbers, they report the disruption of the VWI states, namely the quasi-steady flow seen for smaller Richardson numbers, breaks down into highly disordered localised patches of small vortices. Interestingly, from an order-of-magnitude analysis, they proposed the largest possible size of the Richardson number in VWI. The scaling argument is also closely related to the self-sustaining process (SSP) of coherent structures proposed by Waleffe (1997), and thus the relationship between VWI and SSP will be briefly highlighted later. In Eaves & Caulfield (2015), this result is shown for fixed Reynolds number and thus one of our aims is to confirm the scaling with newly constructed nonlinear equilibrium solutions.

Another more important aim of this work is the theoretical derivation of the scaling of the localised patches seen in the strongly stably stratified case. For the isothermal case, it was found by Blackburn, Hall & Sherwin (2013) in reduced model computations, and by Deguchi & Hall (2014) in Navier–Stokes computations, that coherent vortices seen in the VWI states are vertically localised at large wavenumbers. Subsequently, Deguchi (2015) found that VWI breaks down at very small scales. The new asymptotic regime defines the smallest possible scale of coherent structures comparable to the Kolmogorov scale, and the flow is governed by unit Reynolds number Navier–Stokes equations (UNS). Motivated by that previous work, here we shall show that the UNS theory can be extended to stratified flow, anticipating that the scaling and properties of coherent structures may deviate from VWI as found in the DAL.

We begin our analysis by formulating the problem in the next section. Section 3 concerns the scaling of the nonlinear solutions at the VWI stage. Then the analysis in § 4 shall show that the new, non-VWI, small-scale states can persist for larger Richardson numbers than that given in Eaves & Caulfield (2015) for VWI. Section 5 discusses the implication of our results.

2. Formulation of the problem

Consider a horizontally oriented plane Couette flow configuration with the downward force of gravity g in the Cartesian coordinates (x_*, y_*, z_*). Between the two plates placed at $y_* = \pm h$, a Newtonian fluid is sheared and heated from above. We assume that the velocity $\boldsymbol{u}_* = (u_*, v_*, w_*)$, temperature θ_* and density ρ_* satisfy the boundary conditions

$$u_* = u_0, \quad v_* = w_* = 0, \quad \theta_* = \theta_0 + \theta_1, \quad \rho_* = \rho_0 - \rho_1 \quad \text{at } y_* = h, \tag{2.1a–d}$$

$$u_* = -u_0, \quad v_* = w_* = 0, \quad \theta_* = \theta_0 - \theta_1, \quad \rho_* = \rho_0 + \rho_1 \quad \text{at } y_* = -h, \tag{2.1e–h}$$

and that the fluid has kinematic viscosity ν, thermal diffusivity κ, and coefficient of thermal expansion γ. Here u_0, θ_0, ρ_0, θ_1, ρ_1 are constants. Using the Boussinesq approximation, assuming $\rho_0 \gg \rho_1$, the fluid motion is governed by the Navier–Stokes equations

$$\rho_0(\partial_{t_*} + \boldsymbol{u}_* \cdot \boldsymbol{\nabla})\boldsymbol{u}_* = -\boldsymbol{\nabla} p_* + \rho_0 \nu \nabla^2 \boldsymbol{u}_* - \rho_* g \boldsymbol{e}_y, \quad \boldsymbol{\nabla} \cdot \boldsymbol{u}_* = 0, \tag{2.2a,b}$$

$$(\partial_{t_*} + \boldsymbol{u}_* \cdot \boldsymbol{\nabla})\theta_* = \kappa \nabla^2 \theta_*, \quad \rho_* = \rho_0[1 - \gamma(\theta_* - \theta_0)], \tag{2.2c,d}$$

where $\boldsymbol{\nabla} = (\partial_{x_*}, \partial_{y_*}, \partial_{z_*})$.

If we scale the variables as $t_* = (h/u_0)t$, $(x_*, y_*, z_*) = h(x, y, z)$, $p_* - \rho_0 g y_* = \rho_0 u_0^2 p$, $(u_*, v_*, w_*) = u_0(u, v, w)$, $(\theta_* - \theta_0) = \theta_1 \theta$, and eliminate the density from the equations, we have the non-dimensional equations

$$(\partial_t + \boldsymbol{u} \cdot \boldsymbol{\nabla})\boldsymbol{u} = -\boldsymbol{\nabla} p + Re^{-1} \nabla^2 \boldsymbol{u} - Ra\, Pr^{-1} Re^{-2} \theta \boldsymbol{e}_y, \quad \boldsymbol{\nabla} \cdot \boldsymbol{u} = 0, \tag{2.3a,b}$$

$$(\partial_t + \boldsymbol{u} \cdot \boldsymbol{\nabla})\theta = Re^{-1} Pr^{-1} \nabla^2 \theta, \tag{2.3c}$$

subject to the boundary conditions

$$u = 1, \quad v = w = 0, \quad \theta = 1 \quad \text{at } y = 1, \tag{2.3d–f}$$

$$u = -1, \quad v = w = 0, \quad \theta = -1 \quad \text{at } y = -1. \tag{2.3g–i}$$

Note that $\boldsymbol{\nabla}$ now represents $(\partial_x, \partial_y, \partial_z)$. The system (2.3) is controlled by the Reynolds number, Rayleigh number and Prandtl number, defined by

$$Re \equiv \frac{u_0 h}{\nu}, \quad Ra \equiv -\frac{\gamma g h^3 \theta_1}{\nu \kappa}, \quad Pr \equiv \frac{\nu}{\kappa}, \tag{2.4a–c}$$

respectively. The definition of Ra is the same as that used in Clever & Busse (1992), and thus $Ra < 0$ represents the stable stratification. Since we have assumed that the temperature is proportional to the density, the system is also equivalent to that treated in Eaves & Caulfield (2015). The bulk Richardson number Ri in that paper can be related to the Rayleigh number by

$$Ri \equiv \frac{g h \rho_1}{u_0^2 \rho_0} = -\frac{Ra}{Re^2 Pr}, \tag{2.5}$$

where Eaves & Caulfield (2015) used $(Re, Pr) = (1000, 1)$.

The linear basic flow profile of (2.3) can be found analytically as $[u, v, w, p, \theta] = [y, 0, 0, p_b(y), y]$, where $p_b(y) = P_0 + Riy^2/2$, whilst we must of course use a numerical approach to find nonlinear equilibrium solutions. Here we seek non-trivial steady states. In the periodic domain $x \in [0, 2\pi/\alpha]$, $z \in [0, 2\pi/\beta]$, the flow is discretised by truncated Fourier expansions in x, z, and a Chebyshev expansion in y. After Galerkin projection, we have algebraic equations that can be solved by Newton's method. The basic numerical algorithm is the same as Nagata (1990), Clever & Busse (1992) and a further description of the present code can be found in Deguchi, Hall & Walton (2013).

In the following sections we shall investigate the asymptotic development of the steady solutions at large Re. In the subcritical stratified shear flow study, the range of

the parameters (Re, Ri) at which transition to turbulence could occur, bounded by the critical parameter $Ri = Ri_c(Re)$ say, has been a matter of great concern. The asymptotic analysis of the steady solutions may give, if they can be regarded as a skeleton of turbulence, an important clue for the large Reynolds number development of Ri_c.

Throughout the paper we assume that the solutions have so-called shift–reflect and shift–rotation symmetries

$$[u, v, w, \theta](x, y, z) = [u, v, -w, \theta](x + \pi/\alpha, y, -z), \tag{2.6}$$

$$[u, v, w, \theta](x, y, z) = [-u, -v, w, -\theta](-x, -y, z + \pi/\beta). \tag{2.7}$$

These symmetries were found in the steady wavy instability of the roll convection cell (Clever, Busse & Kelly 1977), and when the thermal effect is absent, the symmetries are identical to those discussed in Nagata (1990).

3. Large-scale structures for small Richardson numbers

Our aim in this section is to confirm the scaling $Ri \sim O(Re^{-2})$ noticed in Eaves & Caulfield (2015), using the computation of nonlinear solutions and formal large Reynolds number asymptotic analysis. In view of (2.5), it is sufficient to show $Ra \sim O(1)$; note that $O(1)$ means $O(Re^0)$ throughout the present paper. Based on the VWI theory, we shall consider the derivation of the scaling using a formal large Reynolds number asymptotic analysis of the fully three-dimensional Navier–Stokes equations. However, since only the streamwise-independent component of the flow, called the 'vortex' in the VWI theory, plays an essential role in deriving the scaling of Ra, we first consider flows independent of x (later we shall see that the balance of the buoyancy term in the x-dependent part is less crucial). The roll-cell found in the unstable Rayleigh–Bénard problem belongs to this class, and it is well known (e.g. from Chandrasekhar 1961) that if we write

$$(u, v, w, p) = (\overline{u}, Re^{-1}\overline{v}, Re^{-1}\overline{w}, p_b + Re^{-2}\overline{p}), \quad \theta = y + Pr\overline{\theta}, \tag{3.1a,b}$$

with $[\overline{\boldsymbol{u}}, \overline{p}, \overline{\theta}](y, z) \in \mathbb{R}$ in (2.3), then we obtain Re-independent equations

$$[\overline{v}\partial_y + \overline{w}\partial_z] \begin{bmatrix} \overline{u} \\ \overline{v} \\ \overline{w} \end{bmatrix} = -\begin{bmatrix} 0 \\ \overline{p}_y \\ \overline{p}_z \end{bmatrix} + (\partial_{yy} + \partial_{zz}) \begin{bmatrix} \overline{u} \\ \overline{v} \\ \overline{w} \end{bmatrix} - Ra \begin{bmatrix} 0 \\ \overline{\theta} \\ 0 \end{bmatrix}, \tag{3.2a}$$

$$\partial_y \overline{v} + \partial_z \overline{w} = 0, \tag{3.2b}$$

$$Pr[\overline{v}\partial_y + \overline{w}\partial_z]\overline{\theta} + \overline{v} = (\partial_{yy} + \partial_{zz})\overline{\theta}, \tag{3.2c}$$

where $(\overline{u}, \overline{v}, \overline{w}, \overline{\theta}) = (\pm 1, 0, 0, 0)$ at $y = \pm 1$. From (3.2*a*) it is now clear that Ra must be an $O(1)$ quantity, to maintain the balance between the viscous and the buoyancy terms. This means that the vortex component in VWI feels the effect of stratification when $Ra \sim O(1)$ and the asymptotic structure is destroyed for larger Ra.

If the fluid is unstably stratified ($Ra > 0$), the vortex equations (3.2) can have a non-trivial solution in their own right. The dashed curve in figure 1 is such a two-dimensional solution branch, computed for $(Re, Pr, \beta) = (5000, 1, 1.905)$. Here, the deviation of the drag on the wall D (i.e. x–z average of $u_y|_{y=1}$) from its laminar value $D = 1$ indicates the presence of nonlinearity. Waleffe (1997) referred to $\overline{u}$ and $(\overline{v}, \overline{w})$ as the streak and roll components, respectively, and here we also adopt that terminology. The roll and temperature components of the two-dimensional solution are exactly the

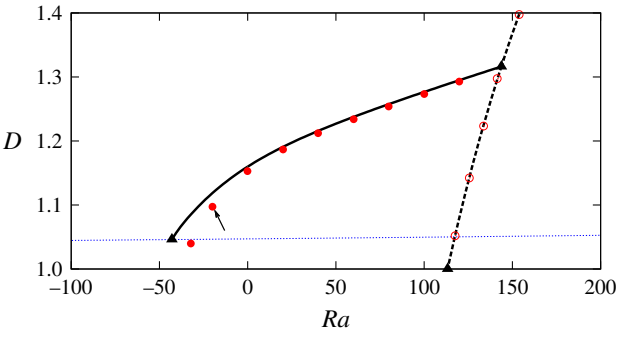

FIGURE 1. (Colour online) Bifurcation diagram of stratified plane Couette flow for $(\alpha,\ \beta,\ Pr) = (0.460,\ 1.905,\ 1)$. Drag D is shown versus Rayleigh number Ra. The thick dashed curve is the two-dimensional roll-cell solution branch for $Re = 5000$; the open circles are the same result but for $Re = 10\,000$. The thick solid curve is the three-dimensional solution branch for $Re = 5000$; the filled circles are the same result but for $Re = 10\,000$. The thin blue dotted curve is the mirror-symmetric solution branch for $Re = 5000$. The bifurcation points for $Re = 5000$ are shown by the triangles.

same as the roll-cell solution found in the Rayleigh–Bénard problem bifurcated at a certain critical Rayleigh number; see Chandrasekhar (1961). The streak component is passively driven by the roll cell, and its magnitude is measured by the drag D.

On the other hand, if the fluid is stably stratified ($Ra < 0$), the thermal effect typically subtracts energy from the roll component, and thus three-dimensionality is essential for sustaining the vortex component via the Reynolds stress. For the isothermal case, Hall & Smith (1991) superimposed a monochromatic wave to support the vortex component. In the same spirit, we add the wave part of the flow

$$\Delta\{(\widetilde{u},\ \widetilde{v},\ \widetilde{w},\ \widetilde{p},\ \widetilde{\theta})\mathrm{e}^{\mathrm{i}\alpha x} + \mathrm{c.c.}\}, \quad [\widetilde{\boldsymbol{u}},\ \widetilde{p},\ \widetilde{\theta}](y,\ z) \in \mathbb{C} \tag{3.3a,b}$$

to $(u,\ v,\ w,\ p,\ \theta)$. Here, $\Delta \ll 1$ describes the amplitude of the wave. More formally, we assume here that the leading-order part in the large Re asymptotic expansion is the sum of (3.1) and (3.3). Substituting the leading-order flow into (2.3) and neglecting the small terms, we have the vortex equations (3.2) and the wave equations

$$\overline{u}\mathrm{i}\alpha \begin{bmatrix} \widetilde{u} \\ \widetilde{v} \\ \widetilde{w} \end{bmatrix} + [\widetilde{v}\partial_y + \widetilde{w}\partial_z] \begin{bmatrix} \overline{u} \\ 0 \\ 0 \end{bmatrix} = -\begin{bmatrix} \mathrm{i}\alpha\widetilde{p} \\ \partial_y\widetilde{p} \\ \partial_z\widetilde{p} \end{bmatrix} - Ra\,Pr^{-1}Re^{-2} \begin{bmatrix} 0 \\ \widetilde{\theta} \\ 0 \end{bmatrix}, \tag{3.4a}$$

$$\mathrm{i}\alpha\widetilde{u} + \partial_y\widetilde{v} + \partial_z\widetilde{w} = 0, \tag{3.4b}$$

$$\overline{u}\mathrm{i}\alpha\widetilde{\theta} + Pr[\widetilde{v}\partial_y + \widetilde{w}\partial_z]\overline{\theta} + \widetilde{v} = 0. \tag{3.4c}$$

If $Ra \sim O(1)$, the wave equations (3.4) become the single equation

$$\left(\frac{\widetilde{p}_y}{\overline{u}^2 - \alpha^{-2}Ri}\right)_y + \left(\frac{\widetilde{p}_z}{\overline{u}^2}\right)_z - \alpha^2\frac{\widetilde{p}}{\overline{u}^2} = 0, \tag{3.5}$$

where $\widetilde{p}_y = 0$ must be satisfied on the walls.

If $Pr \sim O(1)$, then from (2.5), we have $Ri \ll 1$. Therefore, (3.5) reduces to the Rayleigh equation for the streak derived in Hall & Smith (1991). This equation is

inviscid and thus has a singularity at the critical position where $\overline{u}$ vanishes. In the critical layer of thickness $\delta = Re^{-1/3}$ around that position, the viscous effect in the wave equation must be retained, and thus we need a separate analysis there. The analysis of the singularity is essential to understand the mechanism by which the small wave drives the roll. If the critical layer is horizontal, from the Frobenius expansion near the critical position we can see that $\widetilde{p} \sim O(\Delta)$. Then, since $\widetilde{w} \sim O(\delta^{-1}\Delta)$ from the z component of (3.4*a*), we can see that the Reynolds stress driving the roll, which is $O(\widetilde{w}^2)$, is amplified in the critical layer. This stress should balance the viscous term of $Re^{-2}\delta^{-1}$, which is the first derivative of the roll shear stress. (Note that the value of the roll component is continuous across the critical layer and hence what is influenced by the wave is the $O(\delta)$ smaller roll shear stress.) Thus if $\Delta = \delta^{1/2}Re^{-1}$, the concentrated Reynolds stress produces a finite stress jump in the roll across the critical position. It is possible to deduce an analytic form of the jump in terms of $\widetilde{p}$, but since it is identical to that of the VWI theory of Hall & Smith (1991), we do not repeat any further analysis here. If the Richardson number becomes $O(1)$, (3.5) has the form of the Taylor–Goldstein equation for the streak; however for a three-dimensional flow, this is only possible when $Pr \sim O(Re^{-2})$ if $Ra \sim O(1)$. The reason why the wave part less feels the effect of stratification than the vortex part is that the effect of shear advection acting on the wave is much stronger than that acting on the vortex; recall that the vortex component is advected by a small roll velocity component.

A similar tripartite interaction between the roll, streak and wave, has been treated in the SSP theory by Waleffe (1997), but the excitation of the wave was explained by the Orr–Sommerfeld equation rather than the Rayleigh equation. Due to the viscosity remaining in the wave equation, the Reynolds number scaling of the flow field is not fully determined in the SSP framework. In this sense, the reduced description of coherent structures proposed by SSP is considered to be an intermediate reduction of the Navier–Stokes equations to the fully asymptotic VWI approach. However one of the advantages of retaining viscosity is that we can avoid any complication associated with the critical layer singularity: see Hall & Horseman (1991). Recently, Blackburn *et al.* (2013) derived a 'hybrid' model of coherent structures in plane Couette flow using such a regularisation. Subsequently Beaume *et al.* (2015) derived a similar model to analyse a forced flow.

If a stably stratified fluid is subjected to a shear, there is a competition between the stabilisation effect due to the stratification and the destabilisation effect due to the wave instability. As shown in Clever & Busse (1992), this competition leads to a subcritical bifurcation of the three-dimensional solution from the two-dimensional roll-cell solution, and the bifurcated branch can be continued to $Ra < 0$. The solid curve in figure 1 shows the three-dimensional solution branch for $(\alpha, \beta) = (0.460, 1.905)$, corresponding to the 'narrow geometry' used in Eaves & Caulfield (2015). Decreasing Ra from zero, at the other end of the solution branch the flow field acquires a mirror symmetry in the spanwise direction. The mirror-symmetric solution obtained for $Ra = 0$ is identical to the plane Couette flow solutions found in Gibson, Halcrow & Cvitanović (2009), Itano & Generalis (2009): the mirror-symmetric solution branch for $Re = 5000$ is shown by the thin blue dotted curve.

The results shown in figure 1 do not change much for higher Reynolds numbers. For example, the results for $Re = 10\,000$ shown by the points almost overlap with the solid and dashed curves. It should be noted that the collapse of the two-dimensional solution branch is not a surprising result, because it is independent of Re, as remarked earlier. However, in general, the three-dimensional solution does depend on Re, and the asymptotically convergent result seen in the figure can be regarded as a numerical

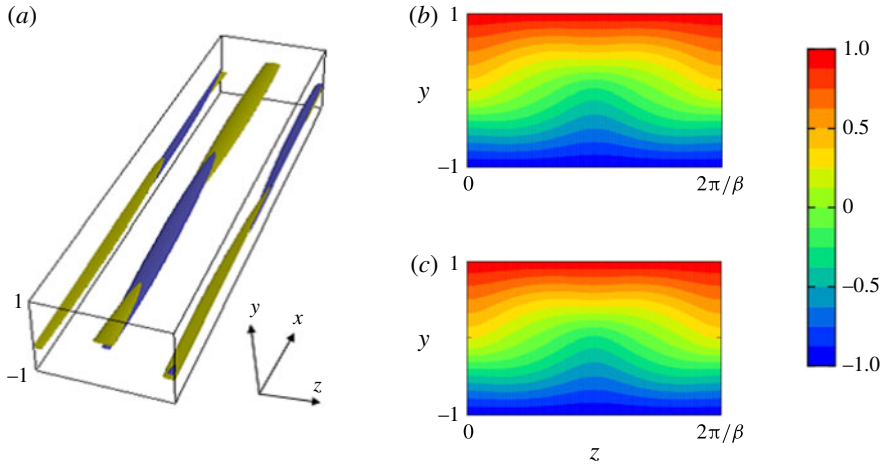

FIGURE 2. (Colour online) The visualisation of the three-dimensional solution indicated by the arrow in figure 1. $(Re, Pr, Ra) = (10\,000, 1, -20)$. (*a*) Yellow/blue is 50 % maximum/minimum isosurface of streamwise vorticity. (*b*,*c*) Streamwise averaged field: (*b*) is the contour of streamwise velocity, streak, whilst (*c*) is the contour of temperature.

confirmation of the scaling given in Eaves & Caulfield (2015). One may notice that the asymptotic convergence of the solutions near the bifurcation point where the mirror-symmetric solution appears is less good. This is because the critical layer becomes nearly flat ($y = 0$) as the bifurcation point is approached, and in this special case the asymptotic structure is modified into a localised structure locally described by the boundary region equations (BRE) as concerned in Deguchi & Hall (2015). In fact, when the mirror-symmetric solution is continued to smaller Ra keeping the computational box size, the flow field naturally develops small-scale vortices localised in both y–z directions, as the asymptotic theory predicts. The readers who are interested in this regime should refer to Olvera & Kerswell (2017), where the similar asymptotic development of the solutions is independently found and more carefully examined numerically. As seen in those observations, small-scale vortices are preferred for larger Ri. In the next section, we consider very large wavenumbers comparable to the intrinsic scale of the smallest vortices, in order to preclude the possibility of localisation in z. In the limit of large wavenumbers it is shown by Deguchi (2015) that both of the VWI and BRE states become the UNS states.

The flow field of the solution indicated by the arrow in the bifurcation diagram is shown in figure 2. Figure 2(*a*) shows the isosurface of the streamwise vorticity, which is a good indicator of the wave component. Figures 2(*b*) and 2(*c*) are the streak and temperature fields, respectively. These pictures are almost identical since for $Pr = 1$ the governing equations for them take the same form at the asymptotic limit. The curved critical layer seen in figure 2(*b*) suggests that the asymptotic limit of this state is governed by VWI (recall that the critical layer position is defined by $\overline{u} = 0$). The location where the wave instability is seen in figure 2(*a*) is in fact the position of the critical layer, as shown for the isothermal cases by Wang, Gibson & Waleffe (2007), Hall & Sherwin (2010).

4. Small-scale structures for moderate Richardson numbers

The disrupted flow in Eaves & Caulfield (2015) is calculated at $Ri = 10^{-2}$, namely $Ra = -10\,000$. Therefore the scenario concerned in the last section, valid for $Ra \sim O(1)$, seems to be inapplicable.

Now let us derive the dependence of the typical scale of the vortex L on Ra. Throughout this section, we select $Pr = 1$, as in Eaves & Caulfield (2015), for the sake of simplicity. As found by Blackburn *et al.* (2013), if we choose the wavenumbers to be $O(L^{-1})$, the VWI states are driven in a layer of vertical thickness $O(L)$. For given L, we can consider the balance of the buoyancy term in the vortex part as we did in the last section. In the vertical momentum equation in the x-averaged part of (2.3*a*,*b*), the viscous–convective balance requires $O(v) \sim O(1/(Re\,L))$, whilst the convective–buoyancy balance yields $O(v^2/L) \sim O(Ra\,Re^{-2}\theta)$. The final key to the scaling is that outside of the layer where the nonlinear vortices are driven, the flow is predominantly the linear basic flow. The matching of the flows in the inner layer and the outer region requires, as we shall see shortly, the quantities u/L and θ/L to be $O(1)$ values. Eliminating v and θ from the viscous–convective balance, the convective–buoyancy balance and $\theta \sim L$, we arrive at $L \sim O(Ra^{-1/4})$.

The length scale represents the maximum size of vortices for a given size of Ra. Thus the size can be related to Ozmidov scale $l_o = (\Phi N^{-3})^{1/2}$ (Ozmidov 1965), where the viscous dissipation rate $\Phi = \nu N^2$ is estimated by the Brunt–Väisälä frequency N. In fact, if we note that the Richardson number can be described as $Ri = (N/S)^2$ using the dimensional shear $S = u_0/h$, the Ozmidov scale can be expressed as $l_o = Ra^{-1/4}h$. At this scale, the effective Richardson number in the roll equations becomes order unity, and thus the viscous–buoyancy balance is achieved. The roll equation is not directly forced by the basic flow shear, see (3.2*a*), and therefore the buoyancy frequency N is the most appropriate choice in estimating Φ.

The localised VWI at each L is self-similar, as shown by Blackburn *et al.* (2013). However, the smaller the L, the smaller the effective Reynolds number felt by the wave is. Therefore, when the effective Reynolds number becomes of order unity, the problem is no longer amenable to the VWI approach. In that case all terms in the Navier–Stokes equations must be retained, as shown by Deguchi (2015). The length scale of this minimal structure is inversely proportional to the square root of the Reynolds number. In fact, it has been shown that this scale corresponds to the Kolmogorov scale $l_k = (\Phi^{-1}\nu^3)^{1/4} = Re^{-1/2}h$ when the dissipation is estimated by the shear as $\Phi = \nu S^2$. This is the scale at which the effective Reynolds number becomes order unity in the wave equations, and thus the viscous–convective balance is recovered. Here the effect of stratification is absent and thus S is used to estimate Φ. If the stratification influences the small scale structure we need to consider the viscous–buoyancy balance as well. In this case we can expect $l_o \sim l_k$, from which we arrive at $Ra \sim Re^2$ (or equivalently $Ri \sim O(1)$).

Now let us rescale the spatial variables as $(x, y, z) = L(X, Y, Z)$. It is easy to see that if we write

$$(u, v, w, \theta) = \frac{1}{Re\,L}\left(U, V, W, \frac{B}{D}\Theta\right), \quad p = \frac{1}{(Re\,L)^2}P, \tag{4.1a,b}$$

then (2.3) becomes the unit Reynolds number Navier–Stokes equations

$$(\boldsymbol{U}\cdot\boldsymbol{\nabla})\boldsymbol{U} = -\boldsymbol{\nabla}P + \nabla^2\boldsymbol{U} - R_0\Theta\boldsymbol{e}_y, \quad \boldsymbol{\nabla}\cdot\boldsymbol{U} = 0, \tag{4.2a,b}$$

$$(\boldsymbol{U}\cdot\boldsymbol{\nabla})\Theta = \nabla^2\Theta, \tag{4.2c}$$

where $\boldsymbol{\nabla} = (\partial_X, \partial_Y, \partial_Z)$ and

$$R_0 = \frac{B}{D}\frac{Ra\,L^2}{Re}. \tag{4.3}$$

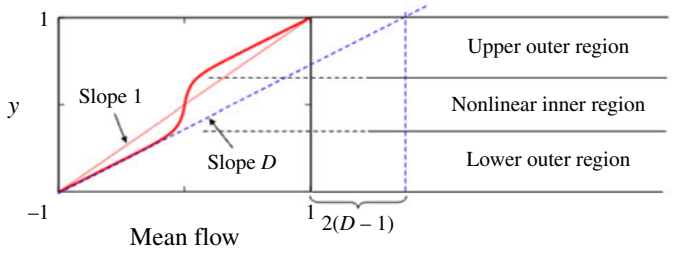

FIGURE 3. (Colour online) Sketch of asymptotic regions for UNS states. The red thick curve is a typical mean flow profile of the corresponding nonlinear solutions. In the inner region with a thickness of $O(Re^{-1/2})$, the nonlinearity creates a velocity displacement of size $2(D-1)$ for the mean flow. The thin red line is the basic flow. The behaviour of the mean temperature is similar.

The factor B/D in (4.1), where B is the Nusselt number (i.e. the x–z average of $\theta_y|_{y=1}$), has been introduced for later convenience. Note that the flow is periodic in $(X, Z) \in [0, 2\pi/\alpha_0] \times [0, 2\pi/\beta_0]$ with the normalised wavenumbers $\alpha_0 = \alpha L$ and $\beta_0 = \beta L$. In the vertical direction we assume that the all nonlinear interaction is confined to $Y \sim O(1)$.

The large $|Y|$ behaviour of the inner flow must be chosen to match the outer flow. Since now we assume there is no nonlinearity in the outer regions, the flow there is simply a linear function, see figure 3. Thanks to the factor B/D in (4.1), we can assume the limiting behaviour of the inner flow takes the form

$$\boldsymbol{U} \to (Y \mp d_0/\beta_0, 0, 0), \quad \Theta \to Y \mp b_0/\beta_0, \quad \text{as } Y \to \pm\infty. \tag{4.4a,b}$$

The displacement of velocity and temperature, d_0/β_0 and b_0/β_0 respectively, are determined by the solution for given α_0, β_0 and R_0. The factor of $1/\beta_0$ in the displacements has been introduced so that the definition of d_0 becomes identical to that used in Deguchi (2015).

In the outer region, the streamwise velocity and temperature take the form

$$u = Dy \pm (1 - D), \quad \theta = By \pm (1 - B), \tag{4.5a,b}$$

where the plus/minus sign must be chosen for the upper/lower outer flow. On the other hand, from the limiting form of the inner flow (4.4), the leading-order outer flow must be

$$u = \frac{1}{Re\, L}\left(\frac{y}{L} \mp \frac{d_0}{\beta_0}\right), \quad \theta = \frac{1}{Re\, L}\frac{B}{D}\left(\frac{y}{L} \mp \frac{b_0}{\beta_0}\right). \tag{4.6a,b}$$

Therefore in order to match (4.5) and (4.6), we require

$$L = (Re\, D)^{-1/2} = Re^{-1/2} + \cdots, \tag{4.7a}$$

$$D = 1 + \frac{1}{Re\, L}\frac{d_0}{\beta_0} = 1 + Re^{-1/2}\left(\frac{d_0}{\beta_0}\right) + \cdots, \tag{4.7b}$$

$$B = 1 + \frac{1}{Re\, L}\frac{b_0}{\beta_0} = 1 + Re^{-1/2}\left(\frac{b_0}{\beta_0}\right) + \cdots, \tag{4.7c}$$

from which we arrive at a length scale comparable to the Kolmogorov scale discussed earlier. The displacement velocity generated by the nonlinear effect modifies the

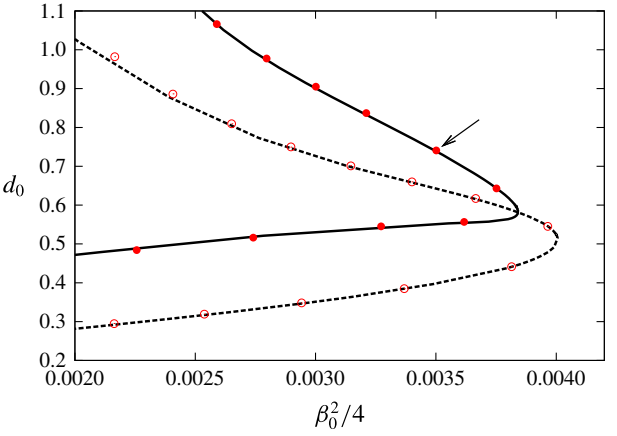

FIGURE 4. (Colour online) The bifurcation diagram of large wavenumber plane Couette flow solutions for $Pr = 1$, $\beta/\alpha = 2$. The normalised displacement velocity d_0 is shown against $\beta_0^2/4$ (that quantity should have appeared in the horizontal axis of figure 2(*c*) in Deguchi (2015)). Here the scaled spanwise wavenumber $\beta_0 \approx Re^{-1/2}\beta$. Curves and points are computed at $Re = 5000$ and $Re = 10\,000$, respectively. Dashed curve: isothermal case $Ra = 0$. Solid curve: stably stratified case $Ra = -0.001Re^2$.

mean flow as shown in figure 3; the displacement can now be expressed as $2(D - 1) = 2Re^{-1/2}d_0/\beta_0$. From (4.7), $R_0 = Ra\,Re^{-2}(1 + \cdots)$, and thus indeed the small-scale structures persist for large negative Rayleigh numbers of $O(Re^2)$, namely $Ri \sim O(1)$.

This result suggests that the Richardson number at $Ri_c(Re)$ may tend to a constant for large Reynolds number. One may notice that this conclusion differs from the previously known results, where it was argued that strongly stratified turbulent flows are governed by a buoyancy Reynolds number $\sim O(Re/Ri)$. If such asymptotic states exist, $Ri_c(Re)$ should ultimately be proportional to Re; see Brethouwer *et al.* (2007), for example. However, their numerical simulations are subjected to certain random forcing to inject energy to the system, and thus the flow configuration is not exactly the same as the one considered in this paper.

In figure 4 we confirm the above scaling in the large wavenumber computation of the steady solution. For the fixed wavenumber ratio $\beta/\alpha = 2$, the value of the normalised displacement d_0 is monitored while changing the scaled wavenumber β_0. Here, the curves and points are computed for $Re = 5000$ and $Re = 10\,000$, respectively. The dashed curve and the open circles are computed for the isothermal case $Ra = 0$; the results are essentially those given in figure 2(*c*) of Deguchi (2015). Similar excellent asymptotic convergence can be found for the stably stratified case $Ra = -0.001Re^2$, shown by the solid curve and the filled circles. The flow structure of the solution at $(Re, Ra) = (10\,000, -100\,000)$, corresponding to the solution indicated by the arrow in figure 4, is shown in figure 5. The streamwise vorticity, streamwise velocity perturbation, and temperature perturbation are localised near the centre of the channel, consistent with the theory described here. In our computation, the perturbation vortices should appear at the centre of the channel due to the symmetry assumed. If there is no symmetry restriction, we may be able to find localised structures for other vertical positions, but such structures are merely a Galilean transformed version of the localised structure seen in figure 5. In fact, similar

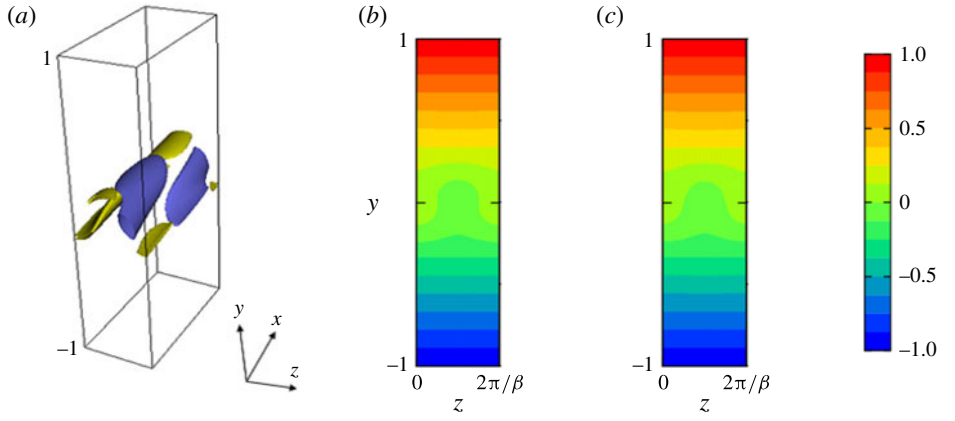

FIGURE 5. (Colour online) The same plot as figure 2 but for the solution indicated by the arrow in figure 4. $(Re, Pr, Ra, \alpha, \beta) = (10\,000, 1, -100\,000, 6.3, 12.6)$.

Ra	Ri	L	Type	$\|u-y\|_\infty$	$\|v\|_\infty$	$\|\theta-y\|_\infty$
$O(1)$	$O(Re^{-2})$	$O(1)$	VWI	$O(1)$	$O(Re^{-5/6})$	$O(1)$
$O(Re^2)$	$O(1)$	$O(Re^{-1/2})$	UNS	$O(Re^{-1/2})$	$O(Re^{-1/2})$	$O(Re^{-1/2})$

TABLE 1. Summary of the large Reynolds number asymptotic analysis ($Pr = O(1)$). Here L is the typical length scale of the vortex and the infinite norm is taken over the computational domain.

to the isothermal cases, our localised solution can be used as a good asymptotic approximation of locally appeared coherent structures in any stratified shear flow, as long as we can assume the background velocity and temperature profiles can be locally approximated by a linear profile.

5. Discussion

We have derived the scaling of coherent structures in stratified plane Couette flow valid for large Reynolds numbers and Prandtl numbers of order unity. Our results are summarised in table 1. The VWI states at large scale persist for $Ri \sim O(Re^{-2})$, as pointed out by Eaves & Caulfield (2015). For larger Ri, the size of the vortices is limited by the Ozmidov scale. At $Ri \sim O(1)$, the size of the vortices reaches the Kolmogorov scale, and the state is governed by the UNS. For larger Ri the viscous and buoyancy effects dominate the flow, and thus for stable stratification self-sustained vortices would be not possible, as both effects subtract energy from the system. This result implies that the laminar–turbulent boundary $Ri = Ri_c(Re)$ seen in numerical simulations and experiments of stratified plane Couette flow approaches a Reynolds number independent constant at sufficiently large Re.

Our investigation has concentrated on the steady solutions. However, it should be noted that the theoretical results here can be extended to time-dependent flows if the appropriate time scale is introduced; for example, it is easy to find for the UNS states that the appropriate time scale is $O(1)$ in t, from the balance of the unsteady term. If we use the dynamical systems theory point of view of turbulence, at large Reynolds numbers the phase space could be subdivided into several regions, each of which

has a distinct asymptotic property. Excursion of the turbulent trajectory in the phase space usually makes the analysis of the scaling very difficult. The nonlinear solutions serve as a way to separate coherent structures of different asymptotic properties, thereby providing a clean confirmation of the theoretical scalings. The analysis here showed that with increasing Ri the asymptotic region governing the large-scale motion 'passes the torch' to that for the smaller scale. The existence region of the solutions in α–β plane has been computed in Deguchi (2015) for the isothermal case, and its development for various Ri is of obvious interest in producing more quantitative results to be compared with experiments/simulations. Such analysis would serve a numerical estimation of the largest possible Ri at which the UNS states can be found. However, this is a computationally quite demanding task and we leave that study for future work.

With this in mind, the theoretical results here seems to be consistent with the previous numerical observations. Recall that the VWI states must satisfy several constraints inherited by the reduced form of the governing equations. The streamwise dependence of the VWI solution is merely a single Fourier mode, that associated with inviscid instability. It is this instability that produces the single unstable eigenvalue of $O(Re^{-1/2})$ seen in the stability analysis of the solution (see Wang *et al.* 2007, Deguchi & Hall 2016), and this is the reason why the DAL at relatively weak stratification produced quasi-steady large-scale states. On the other hand, the UNS regime is less restrictive. There could be several unstable eigenvalues of $O(1)$, which may lead to the disordered transitional fluid motions seen in the DAL for the strongly stratified case. It should also be noted that although the solution shown here has a short periodicity, the UNS theory does not exclude the possibility of the states being localised in all three directions. The plane Couette flow solutions doubly localised in the x–z directions found by Brand & Gibson (2014) for moderate Reynolds numbers seems to strongly support the existence of such UNS states. Since such triply localised states have the smallest kinetic perturbation energy among all possible asymptotic states, their Reynolds number scaling may explain that of the minimal seed of transition to turbulence found by the DAL.

Acknowledgements

After submitting this paper, the author became aware of an independent work by Olvera & Kerswell (2017). The author thanks them for sharing their preprint. Valuable comments made by anonymous referees also are gratefully acknowledged.

REFERENCES

BEAUME, C., CHINI, G. P., JULIEN, K. & KNOBLOCH, E. 2015 Reduced description of exact coherent states in parallel shear flows. *Phys. Rev.* E **91**, 043010.

BLACKBURN, H. M., HALL, P. & SHERWIN, S. 2013 Lower branch equilibria in Couette flow: the emergence of canonical states for arbitrary shear flows. *J. Fluid Mech.* **726**, R2.

BRAND, E. & GIBSON, J. F. 2014 A doubly localized equilibrium solution of plane Couette flow. *J. Fluid Mech.* **750**, R3.

BRETHOUWER, G., BILLANT, P., LINDBORG, E. & CHOMAZ, J.-M. 2007 Scaling analysis and simulation of strongly stratified turbulent flows. *J. Fluid Mech.* **585**, 343–368.

CHANDRASEKHAR, S. 1961 *Hydrodynamic and Hydromagnetic Stability*. Dover.

CLEVER, R. M. & BUSSE, F. H. 1992 Three-dimensional convection in a horizontal fluid layer subjected to a constant shear. *J. Fluid Mech.* **234**, 511–527.

CLEVER, R. M., BUSSE, F. H. & KELLY, R. E. 1977 Instabilities of longitudinal convection rolls in Couette flow. *Z. Angew. Math. Phys.* **28**, 771–783.

DEGUCHI, K. 2015 Self-sustained states at Kolmogorov microscale. *J. Fluid Mech.* **781**, R6.

DEGUCHI, K. & HALL, P. 2014 Canonical exact coherent structures embedded in high Reynolds number flows. *Phil. Trans. R. Soc.* A **372**, 20130352.

DEGUCHI, K. & HALL, P. 2015 Asymptotic descriptions of oblique coherent structures in shear flows. *J. Fluid Mech.* **782**, 356–367.

DEGUCHI, K. & HALL, P. 2016 On the instability of vortex–wave interaction states. *J. Fluid Mech.* **802**, 634–666.

DEGUCHI, K., HALL, P. & WALTON, A. G. 2013 The emergence of localized vortex–wave interaction states in plane Couette flow. *J. Fluid Mech.* **721**, 58–85.

EAVES, T. S. & CAULFIELD, C. P. 2015 Disruption of SSP/VWI states by a stable stratification. *J. Fluid Mech.* **784**, 548–564.

GIBSON, J. F., HALCROW, J. & CVITANOVIĆ, E. 2009 Equilibrium and traveling-wave solutions of plane Couette flow. *J. Fluid Mech.* **638**, 243–266.

HALL, P. & HORSEMAN, N. J. 1991 The linear inviscid secondary instability of longitudinal vortex structures in boundary layers. *J. Fluid Mech.* **232**, 357–375.

HALL, P. & SHERWIN, S. 2010 Streamwise vortices in shear flows: harbingers of transition and the skeleton of coherent structures. *J. Fluid Mech.* **661**, 178–205.

HALL, P. & SMITH, F. T. 1991 On strongly nonlinear vortex/wave interactions in boundary-layer transition. *J. Fluid Mech.* **227**, 641–666.

ITANO, T. & GENERALIS, S. C. 2009 Hairpin vortex solution in planar Couette flow: a tapestry of knotted vortices. *Phys. Rev. Lett.* **102**, 114501.

KAWAHARA, G., UHLMANN, M. & VAN VEEN, L. 2012 The significance of simple invariant solutions in turbulent flows. *Annu. Rev. Fluid Mech.* **44**, 203–225.

NAGATA, M. 1990 Three-dimensional finite-amplitude solutions in plane Couette flow: bifurcation from infinity. *J. Fluid Mech.* **217**, 519–527.

OLVERA, D. & KERSWELL, R. R. 2017 Exact coherent structures in stably-stratified plane Couette flow. *J. Fluid Mech.* (submitted).

OZMIDOV, R. V. 1965 On the turbulent exchange in a stably stratified ocean. *Izv. Acad. Sci. USSR Atmos. Ocean. Phys.* **1**, 861–871.

PELTIER, W. R. & CAULFIELD, C. P. 2003 Mixing efficiency in stratified shear flows. *Annu. Rev. Fluid Mech.* **35**, 135–167.

PORTWOOD, G. D., DE BRUYN KOPS, S. M., TAYLOR, J. R., SALEHIPOUR, H. & CAULFIELD, C. P. 2016 Robust identification of dynamically distinct regions in stratified turbulence. *J. Fluid Mech.* **807**, R2.

WALEFFE, F. 1997 On a self-sustaining process in shear flows. *Phys. Fluids* **9**, 883–900.

WANG, J., GIBSON, J. F. & WALEFFE, F. 2007 Lower branch coherent states: transition and control. *Phys. Rev. Lett.* **98**, 204501.